Color Signal Estimation in High Dynamic Range Scenes

Keita Hirai and Shoji Tominaga
Graduate School of Advanced Integration Science, Chiba University, Chiba, Japan

Abstract

This paper describes a method to estimate color signals in high dynamic range (HDR) scenes. Color signals of incident light into an imaging system consist of the direct spectra of light sources and the indirect spectra of the reflected lights from different object surfaces in a scene. In our study, Wiener estimation method is adopted for reconstructing color signals. The Wiener estimator requires prior statistical information such as the correlation matrix of spectral dataset and the covariance matrix of imaging noise. In Wiener estimation, the fixed matrices of imaging noise and spectral dataset are generally applied to all pixels in an image. However, the imaging noise and spectral dataset are dramatically changed in HDR scenes. Therefore, it is required to determine the suitable estimation matrix for HDR scenes. In this paper, we propose a method for determining suitable noise level and spectral dataset which are applied to Wiener estimation in HDR scenes. For validating our method, experiments using actual HDR scenes are conducted. Experimental results show the proposed method is efficient compared with the conventional Wiener estimation method, and can reconstruct accurate color signal scale in HDR scenes.

Introduction

Spectral analysis of a variety of color signals in a natural scene is definitely one of the most important research problems in the recent color image science and technology [1-5]. This problem often includes (1) acquisition of high dynamic range (HDR) spectral images in outdoor natural scenes and (2) estimation of color signals from the image data [6]. The color signals of incident light into an imaging system consist of the direct spectra of light sources and the indirect spectra of the reflected lights from different object surfaces in a scene. The color signals in an HDR scene have the wide range of luminance level from very dark shadow area to highly bright sky. Therefore the problem of color signal reconstruction requires an HDR technique [7].

So far many estimation methods were proposed for estimating the color signals from image sensor outputs [8–11]. The Wiener estimator is well known and widely utilized for recovering spectral information from noisy observations. This estimator requires prior statistical information such as the correlation matrix of spectral dataset and the covariance matrix of imaging noise. These statistical data significantly affect the estimation accuracy. Therefore there were many attempts to determine suitably the statistical data in advance [12–16].

However, most of the previous works addressed the spectral estimation, not in HDR scenes but in limited dynamic range scenes or low dynamic range (LDR) scenes. Therefore it should be noted that the same estimator with fixed statistical parameters was applied to every pixel of the entire image in a natural scene. On the other hand, HDR scene contains a huge difference in pixel values. So the statistical parameters should be determined dependently on the luminance level of the scene. For instance, the correlation matrix of color signals is determined using two databases of surface-spectral reflectances and light source spectra. In this case, how should we specify the intensity values of light source spectra suitable for the wide range of luminance in an HDR scene? Also the noise characteristics in HDR images are significantly different from the ones in LDR images. We have to determine the noise variance suitably for HDR imaging.

The present paper describes a method for determining the statistical parameters of imaging noises and color signals in order to improve estimation accuracy of color signals in an HDR scene. First, a noise level function is modeled for estimating the noise statistics, which is based on measurements of a LDR scene. This function is then extended to HDR images based on the theory of HDR image synthesis. Second, the database of color signals is created by taking account of luminance values and color temperatures of real light sources. Third, we define the Wiener estimator with variable statistical parameters on noise and color signal properties. An estimation algorithm of color signals is then presented using the improved Wiener estimator. Finally, the feasibility of the proposed method is examined in real HDR scenes.

Imaging System and HDR Image Acquisition

Imaging System

We use an imaging system for capturing multiband images, and a spectro-radiometer for directly acquiring illuminant spectral-power distribution in a particular region of a scene. The imaging system consists of a trichromatic digital camera and two color filters. The camera is a Canon EOS 1Ds Mark II with the image size of 4082 x 2718 pixels, the linear response characteristic and the bit depth of 12 bits. The two additional color filters with different characteristics of spectral transmittance are used for multi-spectral image acquisition. Combining these color filters to the original camera spectral sensitivities leads to different sets of trichromatic spectral sensitivity functions. Therefore, two sets of the modified trichromatic spectral sensitivities result in an imaging system with six spectral bands. Figure 1 shows the overall spectral sensitivity functions of our imaging system.

HDR Image Acquisition

An HDR image is acquired conveniently by combing multiple LDR images captured at different exposure times [7]. Since our imaging system has linear response characteristics, the sensor outputs (pixel values) ρ at two different exposure times satisfy a relationship as

$$\rho^{t(i)}(\mathbf{x}) = \frac{t(i)}{t(j)} \rho^{t(j)}(\mathbf{x}), \tag{1}$$

where $\mathbf{x}$ is the spatial coordinates on an image, $\rho^{t(i)}$ and $\rho^{t(j)}$ are the sensor outputs at exposure times $t(i)$ and $t(j)$. Based on this

relationship, an HDR image can be obtained from LDR images as follows.

$$\rho_{HDR}(\mathbf{x}) = \begin{cases} \rho^{t(1)}(\mathbf{x}) & \left(\rho^{t(1)}(\mathbf{x}) \le \tau\right) \\ \dfrac{t(1)}{t(j)}\rho^{t(j)}(\mathbf{x}) & \left(\dfrac{t(1)}{t(j-1)}\tau < \dfrac{t(1)}{t(j)}\rho^{t(j)}(\mathbf{x}) \le \dfrac{t(1)}{t(j)}\tau\right), \\ \dfrac{t(1)}{t(m)}\rho^{t(m)}(\mathbf{x}) & \left(\dfrac{t(1)}{t(m-1)}\tau < \dfrac{t(1)}{t(m)}\rho^{t(m)}(\mathbf{x})\right) \end{cases} \quad (2)$$

$$j = 2,\ldots,m-1,$$

where ρ_{HDR} is the pixel values of the synthesized HDR image, τ is the threshold for clipping saturated pixels, m is the number of LDR images, and t is exposure time ($t(1) > \cdots > t(m)$). In later experiments, we set $\tau = 3500$.

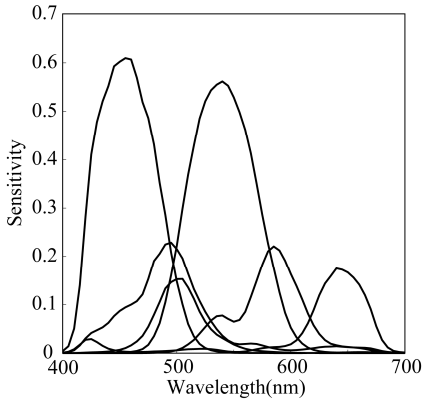

Figure 1. *Spectral sensitivity functions of the six-band imaging system.*

Noise Estimation for HDR Images

Imaging noise is usually assumed as random white noise. A noise variance with a fixed standard deviation is often used for the estimation at all pixels. Strictly speaking, imaging noise is not random white noise [17, 18]. For noise estimation, Tsin et al. showed a CCD camera image pipeline and a generalized noise model [19]. Then, Liu et al. proposed a noise estimation method using a noise level function [20]. However, these previous methods are limited to LDR images. Here we develop first a measurement-based noise level function of an LDR image and then extend this function to HDR images.

Noise Measurement and Noise Level Function

In order to estimate noise characteristics of the present imaging system, we captured one hundred images of known objects, and calculate the average sensor output and the standard deviation at each pixel. The sensor output is described as a sum of signal component and noise component: $\rho = s + n$. First we investigate the dark current at every pixel points of the present imaging system. This measurement is subtracted from each sensor output as a bias term. Then we assumed that the average of noise $\overline{n}$ was zero. Figure 2 shows an LDR scene for the measurements and the noise characteristics. As shown in Fig.2, the noises (standard deviations) in each color channel have linear characteristics to noise-free sensor outputs (average sensor outputs). We can also see no different characteristics among the sensors (color channels). Figure 3 shows the noise characteristics on four types of images which taken by different exposure times. From this result, regardless of the exposure times, the captured images have the same linear characteristic between noises and noise-free sensor outputs.

Now let the signal component s and the noise n be the average sensor outputs $\overline{\rho}$ and the standard deviations σ respectively. Then, based on the noise measurements, we modeled the noise level function of $\overline{\rho}$ as linear model as

$$\sigma = a\overline{\rho} + b, \quad (3)$$

where a and b are the coefficients of the linear noise level function. In actual our imaging system, the coefficients a and b are set as 0.011 and 4.35, respectively. Figure 4 shows the linear noise level function and the actual measurement noise.

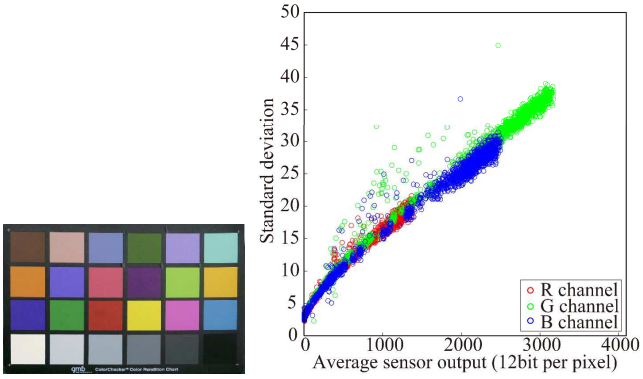

Figure 2. *LDR scene for noise measurement and noise characteristics.*

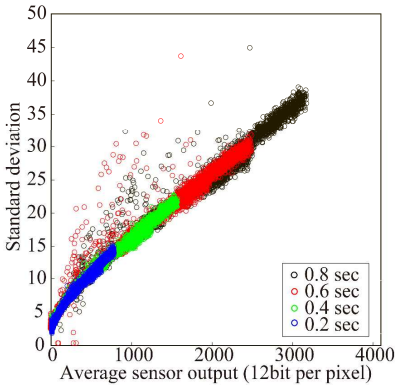

Figure 3. *Noise characteristics at different four exposure times. The exposure times are 0.2, 0.4, 0.6 and 0.8 sec.*

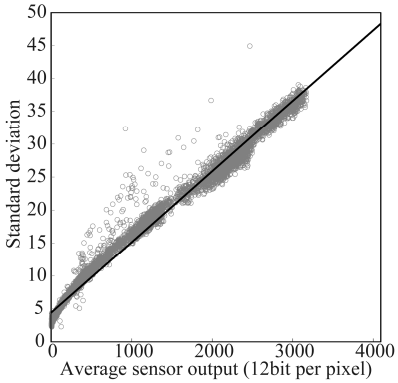

Figure 4. *Noise level function of our imaging system (solod line) and actual measurement noise (scatter plot).*

Extended Noise Level Function for HDR image

HDR images are acquired by replacing the saturated pixels of long exposure images with the ones of short exposure images. In this process, the pixel values of a short exposure image are multiplied by the ratio of the exposure time. This process means that, in the HDR image synthesis, the noise levels increase as well as the sensor outputs (pixel values) shown in Eq.(2). The following equation is the example of noise characteristics of an HDR image synthesized from three LDR images.

$$\sigma_{HDR}(\mathbf{x}) = \begin{cases} \sigma^{t(1)}(\mathbf{x}) & \left(\rho^{t(1)}(\mathbf{x}) \le \tau\right) \\ \dfrac{t(1)}{t(j)}\sigma^{t(j)}(\mathbf{x}) & \left(\dfrac{t(1)}{t(j-1)}\tau < \dfrac{t(1)}{t(j)}\rho^{t(j)}(\mathbf{x}) \le \dfrac{t(1)}{t(j)}\tau\right) \\ \dfrac{t(1)}{t(m)}\sigma^{t(m)}(\mathbf{x}) & \left(\dfrac{t(1)}{t(m-1)}\tau < \dfrac{t(1)}{t(m)}\rho^{t(m)}(\mathbf{x})\right) \end{cases}. \quad (4)$$

Based on this observation, we can assume the noise level function for HDR images as

$$\sigma_{HDR} = a\bar{\rho}_{HDR} + c_t b, \quad (5)$$

where c_t is the ratio of the exposure time, for instance, *t(1)/t(i)* in Eq.(4). The solid line in Fig.5(a) shows the extended noise model for an HDR image synthesized from four LDR images. The scatter plot in Fig.5(a) is the actual measurement noise calculated from one hundred HDR images shown in Fig.5(b). As shown in Fig.5, the estimation using the extended noise level function is efficient, compared with the actual measurement noise from one hundred HDR images.

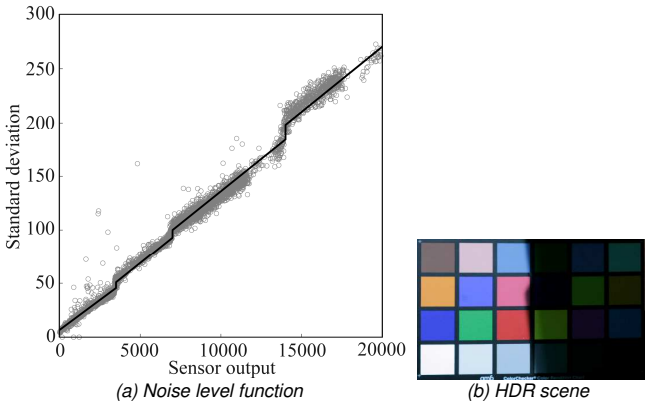

(a) Noise level function (b) HDR scene

Figure 5. *Noise level function for HDR images. The solid line is a noise level function computed from Eq.(5), and the scatter plots are actual measurement noise calculated from one hundred images in HDR scene (b).*

Color Signal Estimation from HDR Images

Overview

Figure 6 shows the overview of our color signal estimation. At first, we obtain the noise-free sensor output **s** and noise **n** by using the noise level function (See the previous section). Next, we calculate the illuminant power scale for determination of suitable color signal database (Described in Section "*Suitable database of color signals for HDR scenes*"). Finally, color signals are reconstructed by the improved Wiener estimation with the correlation matrix of suitable color signal dataset and the covariance matrix of estimated noises (Described in Section "*Improved Wiener Estimator*").

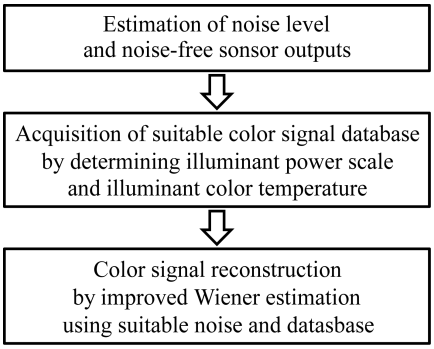

Figure 6. *Overview of our color signal estimation.*

Improved Wiener Estimator

The image sensor outputs are modeled as a following linear system.

$$\begin{aligned} \rho_i(\mathbf{x}) &= \int E(\lambda) R_i(\mathbf{x},\lambda)\, d\lambda + n_i(\mathbf{x}) \\ &= s_i(\mathbf{x}) + n_i(\mathbf{x}), \\ & i = 1,...,6, \end{aligned} \quad (6)$$

where $E(\lambda)$ is the incident color signal into an imaging system, $R_i(\lambda)$ is the spectral sensitivity function of the i-th sensor. In this study we sample all spectral functions at 61 wavelength points in even intervals of 5 nm in the range of [400, 700nm]. Then we can rewrite Eq.(6) in a matrix form:

$$\begin{aligned} \boldsymbol{\rho} &= \mathbf{R}\mathbf{e} + \mathbf{n} \\ &= \mathbf{s} + \mathbf{n}, \end{aligned} \quad (7)$$

where **e** is the 61-dimensional vector representing the color signal $E(\lambda)$, **R** is a diagonal matrix with the size of 6x61 for the spectral sensitivity function, **ρ** is the 6-dimensional sensor output, **n** is the 6-dimensional noise vector, **s** is a 6-dimensional signal which corresponds to the noise-free sensor output.

When color signal **e** and noise **n** are uncorrelated, the estimated color signal $\hat{\mathbf{e}}$ is given by

$$\hat{\mathbf{e}} = \mathbf{C}_{ss}\mathbf{R}^t(\mathbf{R}\mathbf{C}_{ss}\mathbf{R}^t + \boldsymbol{\Sigma})^{-1}\boldsymbol{\rho}, \quad (8)$$

where $\mathbf{C}_{ss}$ is the correlation matrix of color signals and **Σ** is the covariance matrix of noises as follows.

$$\begin{aligned} \mathbf{C}_{ss} &= \mathrm{E}[\mathbf{e}\mathbf{e}^t], \\ \boldsymbol{\Sigma} &= \mathrm{E}[\mathbf{n}\mathbf{n}^t]. \end{aligned} \quad (9)$$

In the estimation, we can assume that the noises in each spectral channel are statistically independent. In this case, the covariance matrix is reduced to be diagonal as

$$\boldsymbol{\Sigma} = \mathrm{diag}(\sigma_1^2, \sigma_2^2, ..., \sigma_6^2). \quad (10)$$

From Eq. (8), Wiener estimation is decided by 3 matrices: **R**, $\mathbf{C}_{ss}$ and **Σ**. In general, **R** and **Σ** are fixed for the imaging system. $\mathbf{C}_{ss}$ is usually calculated from color signal database. In our study, we utilize **Σ** computed from the estimated noises. As described above, we can regard the average sensor outputs $\bar{\rho}$ and the standard

deviations σ as the signal component s and the noise n, respectively. Then by using Eqs.(5) and (6), we can rewrite the extended noise model as follows.

$$\sigma_i = \rho_i - s_i,$$
$$s_i = \frac{\rho_i - c_t b}{1+a}. \tag{11}$$

then,

$$\hat{\sigma}_i = \frac{a\rho_i + c_t b}{1+a}, \tag{12}$$

where, $\hat{\sigma}_i$ is the noises in an HDR image, which are calculated based on the extended noise level function. From Eq.(12), we acquire the noise covariance matrix for HDR images as follow.

$$\mathbf{\Sigma}_{HDR} = diag[\hat{\sigma}_1^{\,2},...,\hat{\sigma}_6^{\,2}]. \tag{13}$$

Suitable database of color signals for HDR scenes

The accuracy of Wiener estimation depends on the statistics of color signal dataset. To determine the correlation matrix **C**ss properly, we used two datasets of surface-spectral reflectances and illuminant spectra.

Figure 7(a) shows a set of 1378 surface-spectral reflectances for natural objects and artificial objects. Figure 7(b) shows an illuminant database consisting of nine light sources, which are the CIE standard spectral-power distributions of daylights with different correlated color temperatures from 5000K to 10000K [18] and the measured spectral-power distribution of daylight by using the spectro-radiometer.

In general, color signal dataset is generated by multiplying the surface-spectral reflectances and the illuminant spectra. However, in HDR scenes, the illuminant power scale and the color temperature significantly affect sensor outputs. Then it is necessary to achieve the suitable illuminant scale and color temperature. For the determination, two-steps algorithms are implemented.

Step 1: Determination of illuminant intensity. The illuminant intensity fitted to the sensor outputs **ρ** determined by the following fitting procedure:

$$\arg\min_{c}\left(\left\|\boldsymbol{\rho}_c - \boldsymbol{\rho}\right\|^2\right),$$
$$\boldsymbol{\rho}_c = \mathbf{s}_c + \mathbf{n}_c = (1+a)\mathbf{s}_c + c_t b, \tag{14}$$
$$\mathbf{s}_c = c\mathbf{R}\mathbf{E}_{6500}\bar{\mathbf{r}},$$

where c is a coefficient for adjusting illuminant intensity, $\mathbf{E}_{6500}$ is a 61x61 diagonal matrix representing the spectra of black body radiator with color temperature 6500K, and $\bar{\mathbf{r}}$ is the average reflectance vector of surface reflectance dataset. We determine the coefficient c to minimize the above fitting error.

Step 2: Determination of color temperature. The color temperature k of illuminant is determined by the following fitting procedure:

$$\arg\min_{\mathbf{E}_k}\left(\left\|\boldsymbol{\rho}_k - \boldsymbol{\rho}\right\|^2\right),$$
$$\boldsymbol{\rho}_k = \mathbf{s}_k + \mathbf{n}_k = (1+a)\mathbf{s}_k + c_t b, \tag{15}$$
$$\mathbf{s}_k = c\mathbf{R}\mathbf{E}_k\bar{\mathbf{r}},$$

where $\mathbf{E}_k$ is the illuminant spectra of k Kelvin.

The illuminant scale factor c and illuminant spectra with suitable color temperature $\mathbf{E}_{sui}$ are determined by the above steps and applied for generating the correlation matrix.

$$\mathbf{C}_{\mathrm{SS_{HDR}}} = \mathrm{E}[(c\mathbf{E}_{sui}\mathbf{r})(c\mathbf{E}_{sui}\mathbf{r})^{\mathrm{t}}]. \tag{16}$$

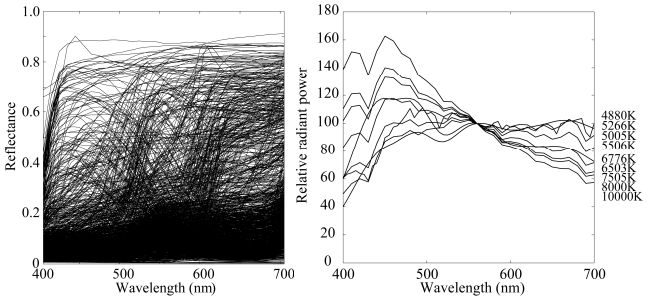

(a) Reflectances (b) Light sources

Figure 7. *Spectral function databases.*

Experiments

Experimental Setups

We used three HDR scenes shown in Fig.8, which include indoor and outdoor HDR scenes. HDR images are synthesized from the LDR images captured using the six spectral band imaging system described in the previous section. Figure 8(c) is an omnidirectional image in a natural scene. The image is captured by a similar imaging system. See Ref.[6] for detail. The red points and squares in the images are the measurement spots by using the spectro-radiometer. The number of measurement spots in Fig.8(a)~(c) are 35, 10 and 10 points, respectively. We also prepared a white reference in the scene and measured the spectra.

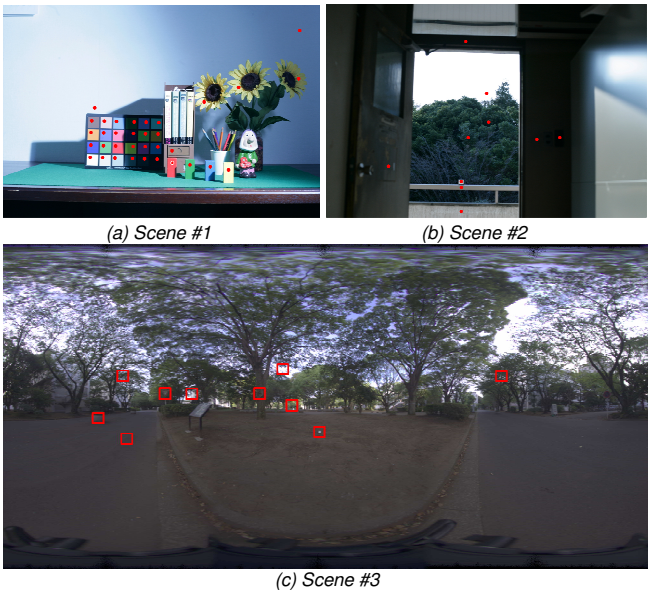

(a) Scene #1 (b) Scene #2

(c) Scene #3

Figure 8. *HDR scenes prepared in our experiments.*

Results and Discussion

For confirming the effectiveness of the proposed method, we estimate the color signals by the conventional Wiener estimation

method. In the conventional estimation, the noise is set at SNR = 40dB, and color signal dataset is generated by multiplying the surface-spectral reflectances and the illuminant spectra shown in Fig.7.

Figure 9 shows the statistical errors of color estimation accuracy. In general, CIELAB color difference is used for evaluating color accuracy. In this calculation, reference white is required. However, when using white reference in HDR scenes, CIELAB color difference often becomes very large values, and it is difficult to understand the color estimation accuracy properly. Therefore, we used normalized root mean square error (NRMSE) [15] instead of CIELAB color difference. Figure 9 shows the NRMSE of the estimated color signals, which is defined by

$$NRMSE = \frac{\sqrt{\left(\mathrm{E}\left\|\mathbf{e}-\hat{\mathbf{e}}\right\|^2\right)}}{\sqrt{\left(\mathrm{E}\left\|\mathbf{e}\right\|^2\right)}}. \qquad (17)$$

As shown in Fig.9, the proposed method is efficient for estimating color signals in HDR scenes, comparing with the conventional Wiener estimation method.

Figure 10 and 11 show the measured and the estimated color signals of Fig.8(b). Since we estimate the color signals in HDR scenes, two types of the horizontal axis scales are represented in Figs.10 and 11, respectively. The red lines in the figures are the color signals of the white reference. In the figures, each measurement or estimated color signal is normalized by the spectral power of each white reference: $\|\mathbf{e}_{white}\|^2 = \|\hat{\mathbf{e}}_{white}\|^2 = 1$. As shown in Figs.10 and 11, the proposed method can reproduce the accurate scales of color signals in HDR scenes, comparing with the conventional Wiener estimation method.

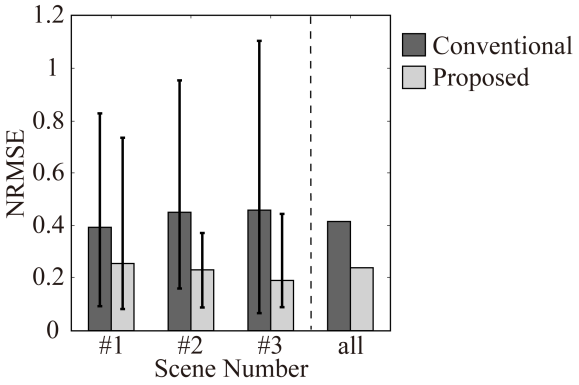

Figure 9. *NRMSE of color signals. Error bars mean the maximum and minimum NRMSE in each scene.*

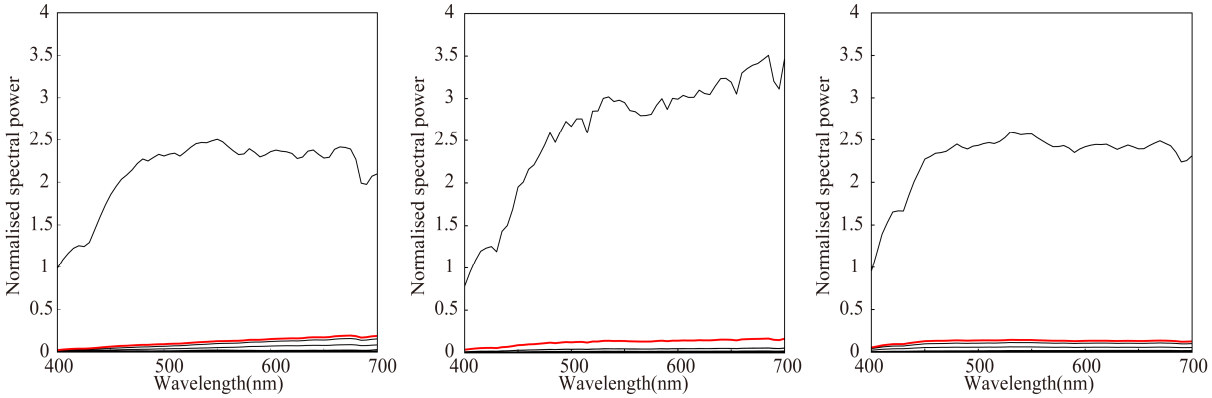

(a) Ground truth (measurement data) *(b) Conventional Wiener estimation* *(c) Proposed Wiener estimation*

Figure 10. *Ground truth and estimated color signals in HDR scene of Fig.8(b). The figures are shown in wide horizontal axis scale. Red lines show the color signals of white reference which is utilized for normalizations.*

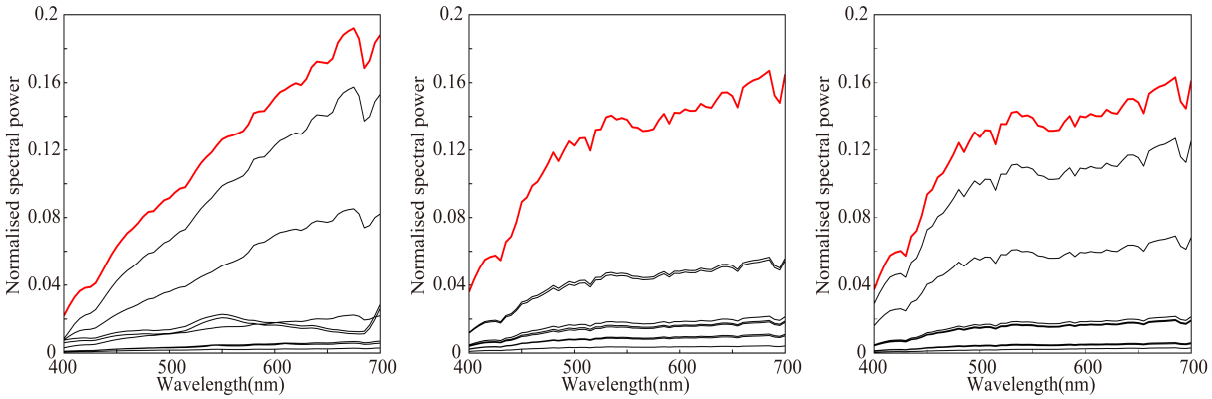

(a) Ground truth (measurement data) *(b) Conventional Wiener estimation* *(c) Proposed Wiener estimation*

Figure 11. *Ground truth and estimated color signals of Fig.8(b). The figures are shown in narrow horizontal axis scale.*

Conclusion

This paper has described a method to estimate color signals in HDR scenes. In particular, our method focuses on the acquisition of suitable imaging noise and spectral dataset in HDR scenes. In the acquisition of the suitable imaging noise, at first, we modeled the noise level function in LDR images as a linear function. Based on the theory of HDR image synthesis, we extended the noise level function for HDR images. In the acquisition of the suitable color signal datasets, suitable power scales and color temperatures of light sources were obtained from sensor outputs. Finally, for reconstructing color signals in HDR scenes, the suitable noise level and color signal database were applied to Wiener estimation. For validating our method, we show the experiments results of the color signal estimations in actual three HDR scenes. The experimental results showed the proposed method is efficient compared with the conventional Wiener estimation method. In particular, the proposed method could reconstruct accurate color signal scale in HDR scene.

In this paper, the noise level function is modeled on the basis of the linearity between sensor outputs and noises. However, there are various types of noise characteristics in practical imaging systems. Then, it is necessary to consider a generalized noise level function for HDR imaging. In addition, we need to improve the two-step algorithm to acquire suitable dataset. Recently, a lot of methods have been proposed to acquire the suitable correlation matrix related with spectral database. Then, for acquiring suitable dataset for HDR scenes, we would like to incorporate the conventional techniques into our method and improve the suitable dataset acquisition algorithm.

References

[1] C.C. Chiao, T.W. Cronin, and D. Osorio, "Color signals in natural scenes: characteristics of reflectance spectra and effects of natural illuminants," J. Opt. Soc. Am. A, **17**(2), 218-224 (2000).

[2] C.C. Chiao, D. Osorio, M. Vorobyev, and T.W. Cronin, "Characterization of natural illuminants in forests and the use of digital video data to reconstruct illuminant spectra," J. Opt. Soc. Am. A, **17**(10), 1713-1721 (2000).

[3] J. Hernández-Andrés, J.L. Nieves, E.M. Valero, and J. Romero, "Spectral-daylight recovery by use of only a few sensors," J. Opt. Soc. Am. A, **21**(1), 13-23 (2004).

[4] E.M. Valero, J. L. Nieves, S.M.C. Nascimento, K. Amano, and D.H. Foster, "Recovering spectral data from natural scenes with an RGB digital camera and colored filters," Color Res. Appl., **32**(5), 352-360 (2007).

[5] O. Kohonen , J. Parkkinen, and T. Jääskeläinen, "Databases for spectral color science," Color Res. Appl., **31**(5), 381-390 (2006).

[6] S. Tominaga, A. Matsuura and T. Horiuchi, "Spectral analysis of omnidirectional illumination in a natural scene," J. Imaging Sci. Technol., **54**(4), 040502-1 - 040502-9 (2010).

[7] E. Reinhard, G. Ward, S. Pattanaik, and P. Debevec, High dynamic range imaging: acquisition, display, and image-based lighting, Morgan Kaufmann (2005).

[8] S. Tominaga, "Multichannel vision system for estimating surface and illuminant functions," J. Opt. Soc. Am. A, **13**(11), 2163-2173 (1996).

[9] P.D. Burns and R.S. Berns, "Analysis of multispectral image capture," Proc. Fourth Color Imaging Conf., 19-22 (1996).

[10] M. Hauta-Kasari, K. Miyazawa, S. Toyooka, and J. Parkkinen, "Spectral vision system for measuring color images," J. Opt. Soc. Am. A, **16**(10), 2352-2362 (1999).

[11] H. Haneishi, T. Hasegawa, A. Hosoi, Y. Yokoyama, N. Tsumura, and Y. Miyake, "System design for accurately estimating the spectral reflectance of art paintings," Appl. Opt., **39**(35), 6621-6632 (2000).

[12] D. Dupont, "Study of the reconstruction of reflectance curves based on tristimulus values: comparison of methods of optimization," Color Res. Appl., **27**(2), 88-99 (2002).

[13] J.M. DiCarlo and B.A. Wandell, "Spectral estimation theory: beyond linear but before Bayesian," J. Opt. Soc. Am. A, **20**(7), 1261-1270 (2003).

[14] H. Shen, P. Cai, S. Shao, and J.H. Xin, "Reflectance reconstruction for multispectral imaging by adaptive Wiener estimation," Opt. Express, **15**(23), 15545-15554 (2007).

[15] Y. Murakami, M. Yamaguchi, and N. Ohyama. "Piecewise Wiener estimation for reconstruction of spectral reflectance image by multipoint spectral measurement," Appl. Opt. **48**(11), 2188-2202 (2009).

[16] N. Shimano, "Noise analysis of a multispectral image acquisition system," Proc. Fifth European Conf. on Color in Graphics, Imaging and Vision (CGIV), 523-528 (2010).

[17] G.E. Healey and R. Kondepudy, "Radiometric CCD camera calibration and noise estimation," IEEE Trans. Patt. Anal. Mach. Intell., **16**(3), 267-276 (1994).

[18] P.D. Burns, "Analysis of image noise in multispectral color acquisition," Ph.D. Thesis, Center for Imaging Science, Rochester Institute of Technology (1997).

[19] Y. Tsin, V. Ramesh, and T. Kanade, "Statistical calibration of CCD imaging process," Proc. IEEE Eighth Int'l Conf. Computer Vision (ICCV), 480-487 (2001).

[20] C. Liu , R. Szeliski , S.B. Kang , C.L. Zitnick , and W.T. Freeman, "Automatic estimation and removal of noise from a single image," IEEE Trans. Patt. Anal. Mach. Intell., **30**(2), 299-314 (2008).

Author Biography

Keita Hirai received the B.E., M.S. and Ph.D. degrees from Chiba University in 2005, 2007 and 2010. He was also a research fellow of Japan Society for the Promotion of Science (JSPS) from April 2009 to March 2010. He is currently an Assistant Professor of Graduate School of Advanced Integration Science, Chiba University, Japan. He is interested in the researches for visual information processing, color image processing, computer vision and computer graphics.